NPG Asia Materials (2013) 5, e45; doi:10.1038/am.2013.11

www.nature.com/am

ORIGINAL ARTICLE

An 'aqueous route' for the fabrication of low-temperature-processable oxide flexible transparent thin-film transistors on plastic substrates

Young Hwan Hwang[1,3], Jin-Suk Seo[1], Je Moon Yun[1], HyungJin Park[1], Shinhyuk Yang[2], Sang-Hee Ko Park[2] and Byeong-Soo Bae[1]

Metal-oxide semiconductors have attracted considerable attention as next-generation circuitry for displays and energy devices because of their unique transparency and high performance. We propose a simple, novel and inexpensive 'aqueous route' for the fabrication of oxide thin-film transistors (TFTs) at low annealing temperatures (that is, $<200\,^{\circ}C$). These results provide substantial progress toward solution-processed metal-oxide TFTs through naturally formed, unique indium complex and post annealing. The fabricated TFTs exhibited acceptable electrical performance with good large-area uniformity at low temperatures. Additional vacuum annealing facilitated the condensation reaction by effectively removing byproduct water molecules and resulted in the activation of the In_2O_3 TFT at low annealing temperatures, even temperatures as low as 100 °C. In addition, we have demonstrated that the flexible and transparent oxide TFTs on plastic substrates exhibit good resistance to external gate bias stress.
NPG Asia Materials (2013) **5,** e45; doi:10.1038/am.2013.11; published online 12 April 2013

Keywords: flexible electronics; oxide semiconductor; solution process

INTRODUCTION

Metal-oxide semiconductors (MOSs) are a unique class of materials that have both transparency and electronic conductivity.[1–3] Increasing demand for transparent semiconducting active materials has resulted in increased attention on the MOSs for next-generation electronics, including electronics for use in high-performance, flexible and transparent applications, because of their favorable field-effect mobility, high optical transparency and good environmental stability.[4,5] In the early studies, these materials were primarily prepared using a vacuum process.[6,7] Although the vacuum-based deposition method has advantages, the high fabrication cost and large-area device uniformity restrict its areas of application. We suggest a simple and novel 'aqueous route' for the fabrication of oxide thin-film transistors (TFTs) at low annealing temperatures (that is, $<200\,^{\circ}C$). These results provide substantial progress toward solution-processed metal-oxide TFTs via a unique indium complex (IC) and post annealing. In addition, we have demonstrated that the flexible and transparent oxide TFTs on plastic substrates exhibit good resistance to external gate bias stress.

The solution-based synthesis approach is considered a promising solution to the issues of fabrication cost and device uniformity. This cost-effective deposition technique can enable the manufacture of electronic circuitry or energy devices that are inexpensive with a wide variety of applications, such as disposable smart radio frequency identification tags, which could replace limited barcodes, or disposable energy-generating devices.[8,9] Moreover, the mild deposition conditions used in the soft process rarely damage the pre-deposited underlying layer, which is an important aspect of the stacked structure.

Despite the substantial benefits and strong potential of the solution-based process, the high processing temperature and hazardous chemicals required in this process hinder its implementation in various fields. The high annealing temperature, which is usually $>400\,^{\circ}C$, is not compatible with flexible plastic substrates, with conventional glass or with the stacked multi-layer structures because of the mismatch in the coefficient of thermal expansion between the layers during deposition.[10–12] A few studies on low-temperature-processable MOSs have been reported.[13–16] However, the authors of these studies used either complex and unstable precursors that required significant effort and multiple steps for synthesis or complicated chemical reactions that are not appropriate for the general fabrication technique. Although methods based on

[1]Department of Materials Science and Engineering, Korea Advanced Institute of Science and Technology, Daejeon, Korea and [2]Oxide Electronics Research Team, Electronics and Telecommunications Research Institute, Daejeon, Korea
Correspondence: Professor B-S Bae, Department of Materials Science and Engineering, Korea Advanced Institute of Science and Technology, 291 Daehak-ro (373-1 Guseong-dong), Yuseong-gu, Daejeon 305-701, Korea.
E-mail: bsbae@kaist.ac.kr
[3]Current address: Printed Electronics Team, Korea Electronics Technology Institute, Jeonju, Korea.
Received 22 May 2012; revised 30 January 2013; accepted 31 January 2013

nanostructures, nanoparticles, nanorods or carbon-related materials also allow low-temperature deposition, concerns about the uniformity of the resulting devices related to the uncontrollable distribution of nanosized materials still remain.[17,18]

Here, we report a novel aqueous route for the fabrication of indium-based metal-oxide thin films as channel layers for TFT applications. The developed aqueous route does not require complex starting materials or chemical reactions. The unique structure of the IC in aqueous solution—naturally born neighboring hexaaquo ions with a centered indium cation—allows for low-temperature oxide formation, sound device uniformity and good storage stability by restricting the hydrolysis and condensation reactions within a solution state. The vacuum post-annealing of the indium oxide (IO) thin film activates the TFT at low temperatures, even temperatures as low as 100 °C. This low-temperature oxide formation provides the realization of a fully transparent TFT on a flexible plastic substrate.

MATERIALS AND METHODS

Precursor synthesis and characterization

All reagents were purchased from Aldrich (St Louis, MO, USA) and were used as received. The precursor solutions for the aqueous route and for the conventional method were prepared by dissolving 0.6 g of $In(NO_3)_3 \times H_2O$ in 10 ml of deionized water or 10 ml of 2-methoxyethanol, respectively. The aqueous solution for the I_7Z_3O TFT was prepared by dissolving 0.42 g of $In(NO_3)_3 \times H_2O$ and 0.18 g of $Zn(NO_3)_2 \times H_2O$ in 10 ml of deionized water. Before deposition of the film, the formulated precursor solution was vigorously stirred for 6 h at room temperature. For the storage stability test, the prepared aqueous solution was stored under ambient atmosphere at room temperature. Raman spectra were measured using a LabRAM HR UV/Vis/NIR. The high-resolution mass spectroscopy (HR-MS; electrospray ionization) analysis was performed using a Bruker Daltonik microTOF-Q II electrospray ionization mass spectrometer (Bruker Daltonik GmbH, Bremen, Germany). Thermogravimetric analysis were performed on 7–10 mg samples that we prepared from the evaporated precursor solution by drying the aqueous precursor solution at 100 °C for 8 h; the thermogravimetric analysis traces were acquired on a TA Instruments Q50 thermogravimetric analyzer (New Castle, DE, USA) using a platinum pan with a heating rate of 5 °C min^{-1} under a dry air flow of 40 ml min^{-1}.

Film fabrication and characterization

The metal-oxide precursor solution prepared via the aqueous route was filtered through a 0.22 μm syringe filter PTFE, GE (Trevose, PA, USA) and spin-coated at 5000 r.p.m. atop the SiO_2/p + Si substrate for 30 s. A 100 nm SiO_2 layer, which served as a gate dielectric, was thermally grown on top of the heavily boron (p +)-doped silicon wafer. After the film was deposited, it was annealed on a hot plate at a given temperature (175, 200, 250 or 300 °C) under an ambient atmosphere for 4 h. The annealing temperature was carefully controlled to prevent overshooting of the desired temperature. The temperature of the hotplate was stabilized for 1 h before the device was annealed, and the device was annealed directly on the hotplate under ambient atmosphere. For the vacuum-annealed devices, additional vacuum annealing was applied to In_2O_3 thin films previously annealed at 100 °C for 4 h under ambient atmosphere; the additional annealing step consisted of the device being heated in a rapid thermal annealing system for 30 min at 100 and 125 °C under a pressure of 5×10^{-2} atm. To control the temperature accurately and avoid overshooting, a two-step procedure for increasing the temperature was adopted. X-ray diffraction patterns were recorded using a RIGAKU D/MAX-2500 equipped with a Cu Kα radiation source coupled to a multilayer mirror. X-ray photoelectron spectroscopy (XPS) spectra were measured using a Thermo VG Scientific Sigma Probe (Waltham, MA, USA) with a base pressure of 1×10^{-10} Torr (ultra high vacuum), and monochromated Al Kα radiation (1486.6 eV) was used. The surfaces were cleaned using Ar-ion sputtering under conditions of 1 kV and 1 μA for 30 s before the XPS measurements. High-resolution cross-sectional transmission electron microscopy images and selected area diffraction patterns were obtained using a JEM-2100F (HR) (JEOL, Tokyo, Japan) with an electron acceleration voltage of 200 kV. Ultraviolet–visible spectra were recorded using a Shimadzu UV310PC UV–VIS–NIR spectrophotometer (Shimadzu, Kyoto, Japan).

TFT fabrication and electrical measurements

The final 100 nm Al source and drain electrodes were deposited using an e-beam evaporator (pressure $\sim 10^{-6}$ Torr) for 1000 μm × 100 μm (common gate with p + Si) through a shadow mask. The electrical performance of the devices fabricated on wafers was measured under ambient atmosphere using an HP 4156A precision semiconductor parameter analyzer (HP, Santa Clara, CA, USA). The saturation mobility was extracted from the transfer characteristics using the following equation:

$$I_D = \frac{WC_i}{2L}\mu_{sat}(V_G - V_{th})^2$$

where C_i, W and L are the capacitance of the gate dielectric per unit area, the channel width and the channel length, respectively. The sub-threshold slope was calculated as the minimum value of the inverse slope of the plot of $\log_{10}(I_D)$ versus V_G.

Fabrication and performance of transparent In_2O_3 TFT on flexible polyethylene naphthalate (PEN) substrates

The modified PEN substrates were laminated on carrier glass substrates using a cool-off-type adhesive (Intelimer) for glass-like processes. The hybrid buffer layers were deposited to create a smooth surface with low water permeation. The 150 nm thick In-Sn-O (indium tin oxide) gate electrode was deposited at room temperature by radio frequency magnetron sputtering. The Al_2O_3 gate dielectric was prepared using the atomic layer deposition technique at 150 °C to a depth of 176 nm using trimethyl aluminum and water as an Al source and as an oxygen precursor, respectively. The indium tin oxide source and 150 nm drain electrode were grown using radio frequency magnetron sputtering at room temperature. The active IO film was deposited via a spin-coating method with a spin speed of 5 k.r.p.m. for 30 s; the film was subsequently annealed on a hot plate at 200 °C for 4 h. The IO semiconductor thin film was patterned using a diluted hydrogen fluoride solution (1:150) for 35 s. The Al_2O_3 protective layer was grown to preserve a clean interface at 180 °C via atomic layer deposition using the same precursors. After the fabrication process, the temperature was decreased to < 10 °C to detach the flexible device from the carrier substrate. Finally, the flexible device was annealed at 170 °C under an O_2 atmosphere. The electrical performance measurements were performed in a dark box using an Agilent B1500A semiconductor parameter analyzer (Agilent, Santa Clara, CA, USA). Positive and negative gate bias stresses were applied for 10 ks in the dark and under room temperature conditions to measure the stability characteristics (S/D electrodes were grounded during the gate bias stress).

RESULTS AND DISCUSSION

The combination of indium nitrate and water as a precursor and solvent, respectively, provides a simple and unique structure of IC in a solution state. The water behaves as a solvent with a high static dielectric constant (that is, > 80), which favors the dissociation of ionic species and also acts as a σ-donor molecule that reacts as a nucleophilic ligand.[19] When the indium precursor is dissolved in water, the ionized indium cation, In^{3+}, is solvated by the neighboring water molecules.[19,20] As the electronegativity, coordination number and valence number of In are 1.78, 6 and 3 + , respectively, we speculated that the stable form of the IC in water is one in which the IC is coordinated with hexaaquo ions that, at low pH values, have a centered indium cation.[21,22] The Raman spectrum of the aqueous solution, displayed in Figure 1a, indicated the formation of $[In(OH_2)_6]^{3+}$. The peak centered at 485 cm^{-1} is attributed to the totally symmetric In–O stretching vibrations, which provide evidence of the expected structure.[21] The peak observed at 720 cm^{-1} is attributed to free nitrate ions, which do not participate in the formation of the complex.

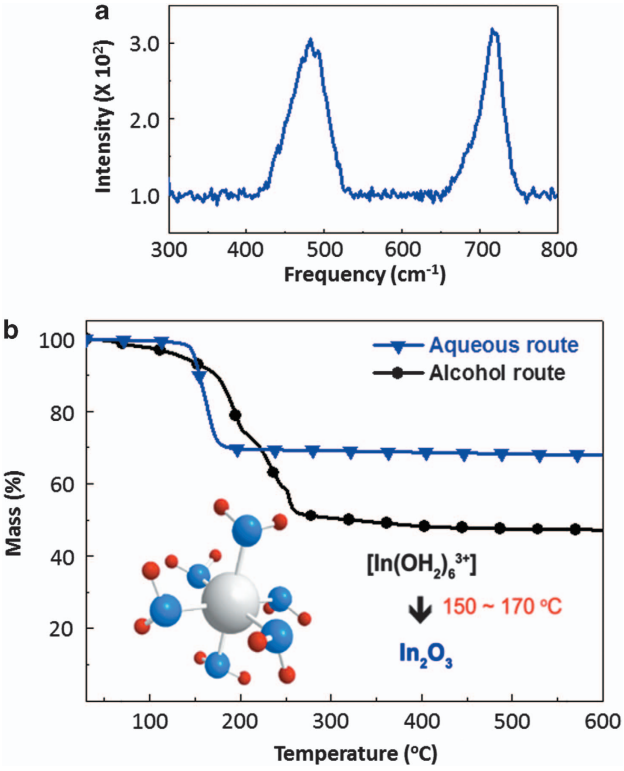

Figure 1 Structure and thermal analysis of the aqueous- and conventional 2-methoxyethanol-based solutions. (**a**) Raman (300–800 cm^{-1}) spectrum of the aqueous solution. (**b**) Thermogravimetric analysis traces of the aqueous- and 2-methoxyethanol-based solutions used for the deposition of In_2O_3 thin films. The aqueous solution and 2-methoxyethanol solution are denoted by blue (reverse triangles) and black (circles) lines, respectively. The chemical structure in the inset represents the proposed indium complex in aqueous solution.

The HR-MS analysis of precursor solutions with indium nitrate dissolved in water and 2-methoxyethanol was followed to understand the structure of the IC in different cases, as shown in Supplementary Figure S1. According to the HR-MS analysis, the mass spectrum of the aqueous solution contained several peaks, located at 200–300, whereas the spectrum of the 2-methoxyethanol solution contained only two discrete peaks. The molecular weights of the majority of the chemical species were 204.90, 222.91, 240.90 and 257.91. The difference in these molecular weights was 18, which is identical to the molecular weight of an aquo ion. This result implies that several types of chemical species with different numbers of neighboring water molecules were detected in the HR-MS analysis. As the coordination number of the indium atoms is fixed at 6 and because a symmetric chemical structure is also indicated by the Raman study, the structure of the IC in an aqueous solution state can be reasonably concluded to be monomeric $[In(OH_2)_6]^{3+}$, which indicates no presence of nitrate ions in the complex. The expected chemical structure is $In(OH_2)_6$, and nitrate ions are not significantly ionically bonded with the In cations but are rather dispersed or coordinated with water molecules. As such, the nitrate ions form HNO_3 molecules (which exhibit a boiling temperature of 83 °C in a dilute nitric acid solution) in a solvated state in water, and the different structure results in different thermal decomposition behavior compared with the chemical structure of pristine $In(NO_3)_3 \times H_2O$ purchased from Aldrich. The other chemical species observed in the HR-MS study are attributed to the debonding of coordination bonds between the indium cation and the neighboring aquo ions (with molecular weights of <222.91) during the measurement and/or the physically adsorbed water (with molecular weights of >222.91) from the actual IC.

The thermogravimetric analysis traces of the precursor solutions, displayed in Figure 1b, indicate that the thermal decomposition temperature was substantially decreased in the aqueous route. The thermal decomposition of the aqueous solution was completed at approximately 170 °C, whereas the decomposition temperature of the 2-methoxyethanol solution was >230 °C. The low-temperature thermal decomposition behavior of the aqueous solution is strongly related to the unique structure of the IC. As the coordination bond between the cation and neighboring aquo ion is relatively weak, it is easily broken with low thermal energy compared with the covalent bonds in the 2-methoxyethanol-based precursor.

The chemical evolution of IO thin films according to the annealing temperature was investigated using XPS, as shown in Figures 2a and b. Although metal hydroxide species may have been converted to oxides via an input of external energy, the surface was cleaned by Ar-ion sputtering to avoid carbon contamination. During the solution process used for metal-oxide thin films, metal hydroxides underwent a gradual conversion to metal oxides through either a thermally driven condensation reaction or direct oxidation upon thermal annealing.[23,24] The conversion of the IC to IO is clearly demonstrated in Figure 2c. At the early stage of annealing, thermally driven hydrolysis occurs. As the annealing temperature is increased, the condensation reaction via oxolation and olation occurs, which is assisted by external energy. Peaks attributable to impurities, such as hydroxide- and nitrate-related species, appear at approximately 533 and 534 eV, respectively.[25,26] These impurities are observed in films annealed at 175 and 200 °C that were fabricated from the 2-methoxyethanol-based solution. The N and C 1s XPS analysis, displayed in Supplementary Figure S2, indicates that both nitrate- and carbon-related species are also observed in the same films. Apparently, the residual organic impurities and nitrate-related species interrupt the formation of oxides at low temperature and require high thermal energy for decomposition and oxide formation in a 2-methoxyethanol-based approach.

In the case of the aqueous precursor solution, its simple chemical structure enables the preparation of IO at low temperatures. Most of the hydroxide- and nitrate-related species disappear upon annealing at 175 °C, whereas a large amount of them are still observed in films prepared from the 2-methoxyethanol solution. As the primary driving force for the construction of oxide frameworks is condensation, which is a hydroxide-consuming process, the observation of chemical species is an effective way to describe the formation of IO. Figure 2c describes the aforementioned chemical evolution according to the annealing temperature. A distinct increase in these species is observed at approximately 175 °C, where the IO species govern the film composition, whereas a relatively small amount of IO species are observed in films annealed at 150 °C. The quantity of oxygen vacancies is similar over the entire temperature range. The nitrate-related peak is only observed in the spectra of films annealed at 100 °C and is rarely observed in the spectra of any other films. The N 1s XPS, shown in Supplementary Figure S3, also illustrates a similar behavior in that nitrate species are detected in the films annealed at 100 °C and small amounts of them are found in films annealed at 150 °C.

These results indicate that nitrate anion groups are more easily eliminated, even at 150 °C, with low-temperature thermal annealing than are chloride or other organic-based precursors. According to the XPS analysis, 175 °C is a sufficient temperature for IO formation from

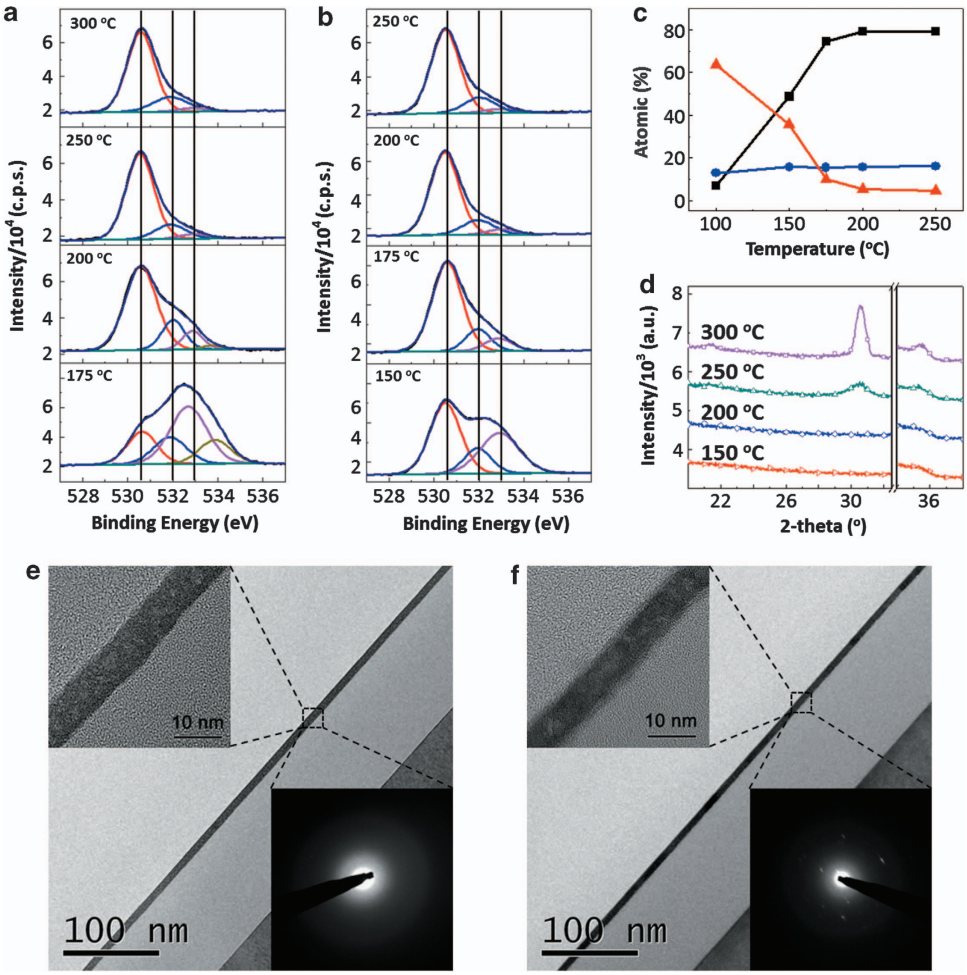

Figure 2 Surface analysis of In_2O_3 films deposited using aqueous- and conventional 2-methoxyethanol-based solution. (**a**, **b**) X-ray photoelectron spectroscopy (XPS) O 1s analysis of a In_2O_3 thin film according to the deposition temperature prepared using a conventional 2-methoxyethanol-based solution (**a**) and the aqueous solution (**b**) (530.5 eV: O in oxide lattices without vacancies, 532.0 eV: O in oxide lattices with vacancies, and 533 eV: O in hydroxide-related species). (**c**) Compositional analysis of In_2O_3 thin films prepared via the aqueous route (■: O in oxide lattices without vacancies, ●: O in oxide lattices with vacancies, and ▲: O in hydroxide-related species). (**d**) X-ray diffraction patterns of In_2O_3 thin films. (**e, f**) High-resolution transmission electron microscopy cross-sectional images of In_2O_3 thin films prepared via the aqueous route and annealed at 200 °C (**e**) or 250 °C (**f**).

the aqueous precursor solution, whereas a much higher thermal energy is required for the 2-methoxyethanol-based solution.[27,28]

The x-ray diffraction patterns of IO thin films, as shown in Figure 2d, verify the formation of the desired IO thin films, which were fabricated from the aqueous precursor solution. The prepared IO thin films remain in an amorphous phase until the temperature reaches 200 °C, and crystallization occurs above 200 °C. The transmission electron microscopy images and selected area diffraction patterns of films annealed at 200 and 250 °C, as shown in Figures 2e and f, show that the IO films have a very smooth surface with an almost amorphous structure (transmission electron microscopy images and selected area diffraction patterns for films annealed at 100, 150 and 300 °C are displayed in Supplementary Figure S4). The partially crystalline structure in the high-resolution image and in the selected area diffraction pattern of an IO film annealed at 250 °C also indicates that the crystallization begins at that temperature.

The transfer characteristics of IO TFTs prepared from 2-methoxyethanol- and aqueous-based solutions are displayed in Figures 3a–e, respectively (output characteristics and stability test of aqueous IO TFTs are shown in Supplementary Figures S5 and S6, respectively). The IO TFT prepared via the aqueous route is activated when annealed at 175 °C under ambient atmosphere, whereas a far greater temperature is required to activate the IO TFT prepared from the 2-methoxyethanol-based solution. This result is in accord with the aforementioned observation that the formation of an IO active layer through annealing at 175 °C is sufficient. Indium zinc oxide (IZO) TFTs were also fabricated to diversify the application area and to enhance the stability of a device prepared via an aqueous route. The transfer characteristics of IZO TFTs are shown in Figures 3f–h (electrical performance of IZO TFTs with various compositions are displayed in Supplementary Figure S7). The carrier concentration of IO thin films is well known to be easily controlled through the addition of different-sized metal cations, that is, Zn, Ga and Al.[2] These cations usually grant an amorphous property to the thin film, which is an important aspect when considering the uniformity of a large-area device. An aqueous route allows for the preparation of IZO TFTs at a lower temperature compared with that used in the previously reported 2-methoxyethanol-based approach.[10–12]

To investigate the uniformity of the devices, 36 TFTs with an IO active layer prepared via the aqueous route were fabricated at an

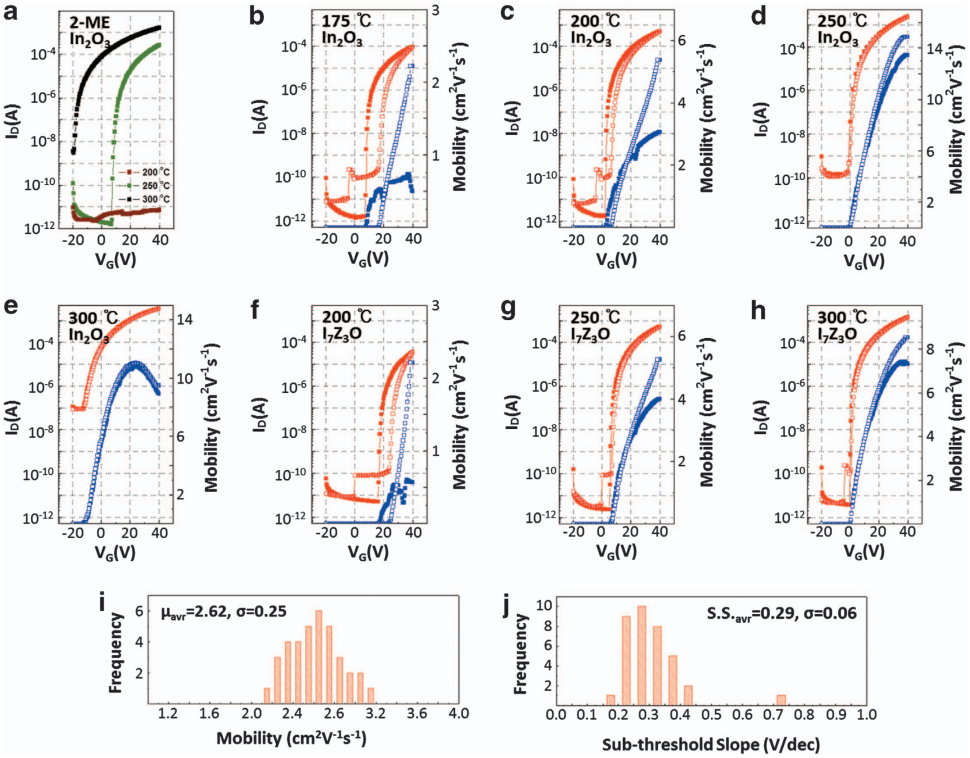

Figure 3 Thin-film transistor (TFT) performance of metal-oxide TFTs prepared from aqueous- and conventional 2-methoxyethanol-based solutions at different annealing temperatures. (Red: drain current; blue: extracted field-effect mobility as a function of the gate voltage; channel length, $L = 100\,\mu m$, channel width, $W = 1000\,\mu m$). The transfer characteristics were measured with a source-drain voltage of 40 V on a 100 nm SiO_2/p+ Si substrate. (**a**) In_2O_3 TFTs according to the annealing temperature used in their preparation from the 2-methoxyethanol solution. (**b**–**h**) In_2O_3 (**b**–**e**) and I_7Z_3O (**f**–**h**) TFTs prepared from the aqueous precursor solution. (**i**, **j**) Histogram of the mobility (**i**) and sub-threshold slope (**j**) for 36 In_2O_3 TFTs (6 × 6 array) processed at 200 °C and prepared from the aqueous precursor solution.

annealing temperature of 200 °C. The TFTs exhibited similar performances, with a low standard deviation of mobility ($\mu = 2.62 \pm 0.25$ $cm^2\,V^{-1}\,s^{-1}$) and sub-threshold slope ($S = 0.29 \pm 0.06$ V/decade), as shown in Figures 3i and j. The transfer characteristics of the 36 TFTs, represented in Supplementary Figure S8, indicate that the turn-on voltage is approximately 0 V. An abnormally high S.S. of approximately 0.7 V/decade for one of the TFTs originated from contamination during the fabrication process. These results imply that the TFTs fabricated via the aqueous solution process have good device uniformity and yield.

The storage stability of a precursor solution is an important issue in sol-gel chemistry. The TFTs fabricated from pristine and 100-day-old aqueous solutions were compared with investigate the storage stability of the aqueous solution. The TFTs showed similar transfer characteristics, as shown in Supplementary Figure S9. The good uniformity and storage stability arose from the unique chemical structure of the IC. The neighboring aquo ligand prevented chemical reactions, hydrolysis and condensation in the aqueous solution state. In addition, the easily decomposable adjoining aquo ligand enabled the use of low annealing temperatures, which were substantially lower than those used in previous reported investigations.

Vacuum annealing is a proficient method to eliminate gaseous products during chemical reactions.[29] As condensation reactions via olation and oxolation involve the liberation of water molecules, the effective removal of water molecules facilitates the forward reaction.[20] The XPS O 1s spectrum of IO thin films annealed at low temperatures, shown in Figure 4a, reveals that a large amount of indium species combine with hydroxide-related species when the film is annealed under an ambient atmosphere at only 100 °C. Vacuum post annealing (at 100 and 125 °C) was applied to the same film for the purpose of promoting oxide formation at low temperatures. The XPS O 1s analysis indicates that the vacuum annealing results in the removal of impurities and promotes condensation that effectively converts the unreacted indium-hydroxide-related species to IO species. The chemical composition of the IO thin film annealed at 100 °C under ambient conditions is governed by the hydroxide-related species. As a consequence of vacuum annealing, the forward reaction is facilitated, and the formation of oxide is achieved using a low-temperature process. The nitrate-related species, which usually impede the oxide formation process, are also removed during the vacuum post-annealing process.[20] The vacuum annealing also enables the generation of charge carriers with low thermal energy, whereas ambient annealing conditions require much greater thermal energy.[30] The electrical performance of the TFTs is in accord with the aforementioned observation that the vacuum-post-annealed IO TFT is activated by a low-temperature process, even at temperatures as low as 100 °C. The output and transfer characteristics of vacuum-post-annealed IO TFTs are shown in Figures 4b–e. The TFTs post-annealed under vacuum at 100 °C and 125 °C exhibited average mobilities of 0.55 and 2.43 $cm^2\,V^{-1}\,s^{-1}$, respectively, and sub-threshold slopes of 0.86 and 0.57 V/decade, respectively (Supplementary Figures S10 and S11). The stability of the devices was also invested, and the results are displayed in Supplementary Figures S12 and S13.

The representative advantage of MOSs is their transparency. As the transmission of light and electrical conductance are contradictory properties, no materials other than metal oxides offer both

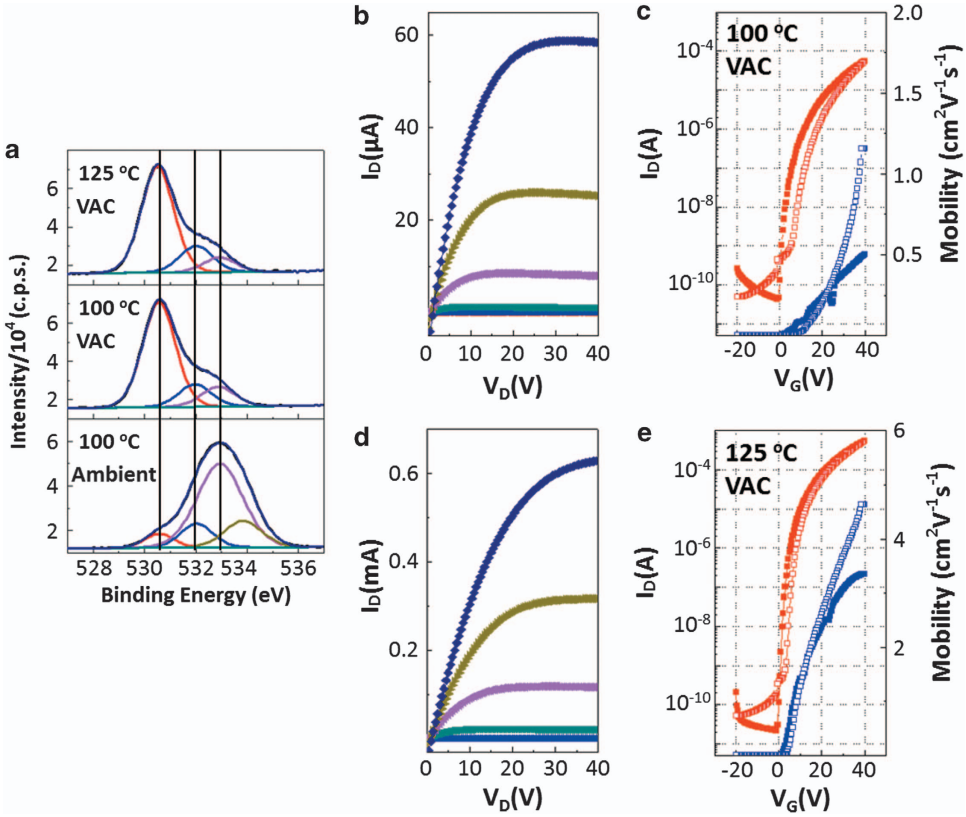

Figure 4 Vacuum-post-annealed In_2O_3 thin-film transistors (TFTs) prepared using the aqueous precursor solution. (**a**) XPS O 1s analysis of the same In_2O_3 thin film annealed at 100 °C under ambient atmosphere, post-annealed at 100 °C under vacuum, and post-annealed at 125 °C under vacuum. (**b**–**e**) Output characteristics (**b**, **d**) and transfer characteristics (**c**, **e**) of In_2O_3 TFT deposited on a 100 nm SiO_2/p+ Si substrate from the aqueous precursor solution and post-annealed under vacuum at 100 °C and 125 °C, respectively.

transparency and semiconducting properties simultaneously.[1] The transparency and amorphous properties, which provide resistance to cracking or cleavage, make metal-oxide TFTs suitable for use in flexible electronics. A transparent IO TFT annealed at 200 °C was implanted on a flexible PEN substrate; optical images and a schematic of the device's structure are displayed in Figure 5a. The electrical performance, including output characteristics, transfer characteristics and stability, of the IO TFT are shown in Figures 5b–d. The finalized transparent TFT on the flexible PEN substrate exhibited good electrical mobility ($\mu = 3.14\,cm^2\,V^{-1}\,s^{-1}$), a sub-threshold slope (S.S. = 158 mV/decade), and an on-to-off current ratio $>10^9$. The IZO TFT on a polyimide substrate, where the TFT was annealed at 250 °C, showed a slightly improved electrical performance because of the improved interface and improved material issues: $\mu = 4.03\,cm^2\,V^{-1}\,s^{-1}$, S.S. = 145 mV/decade, and $I_{on/off} > 10^9$. The transfer characteristics and stability of IZO TFT are displayed in Figures 5e and f.

As the active layer was passivated with a thin Al_2O_3 (9 nm), the effective dimension of the interface area between the active layer surface and atmosphere became small. In addition, no hysteresis was observed in the resultant electrical characteristics and the device showed hard saturation behavior. The better interface between the IO semiconductor and the Al_2O_3 gate insulator also affected the hysteresis.[31] The gate bias stability is an important parameter in the assessment of materials and devices for further integrated applications. Resistances to positive gate bias stressand to negative gate bias stress are highly desirable for display applications. The shifts in the transfer characteristics with positive gate bias stress for an IO transparent TFT (PEN) and a IZO TFT (polyimide) are shown in Figures 5d and f. They shift to positive voltages of 1.47 (IO) and 0.29 (IZO) V with 10 ks of stress. The electrical performance modulation that arises from negative gate bias stress, as displayed in Supplementary Figure S14, is smaller than that of positive gate bias stress: 0.5 V for IO and 0.12 V for IZO TFT with 10 ks of stress. The resulting turn-on voltage shift, summarized in Figure 5g, indicates that the flexible TFTs prepared via the aqueous route are stable under bias stress and that their stability is comparable to that of vacuum-processed devices.

CONCLUSIONS

In conclusion, we have developed a novel aqueous route to fabricate low-temperature-processable MOSs. The thermogravimetric analysis and XPS analyses indicated that oxide formation is achieved at low temperatures (that is, as low as 175 °C), whereas conventional alcohol-based routes requires far greater temperatures. An amorphous IO thin film was obtained upon annealing at 175 °C, and the TFT prepared using the film as an active layer exhibited good performance. The optimized IO TFT, which was annealed at 200 °C, exhibited good uniformity and good electrical performance: $\mu = 2.62 \pm 0.25\,cm^2\,V^{-1}\,s^{-1}$ and S.S. = 0.29 ± 0.06 V/decade, with a turn-on voltage of 0 V. Additional post-annealing under vacuum facilitated the condensation reaction by effectively removing byproduct water molecules, and the

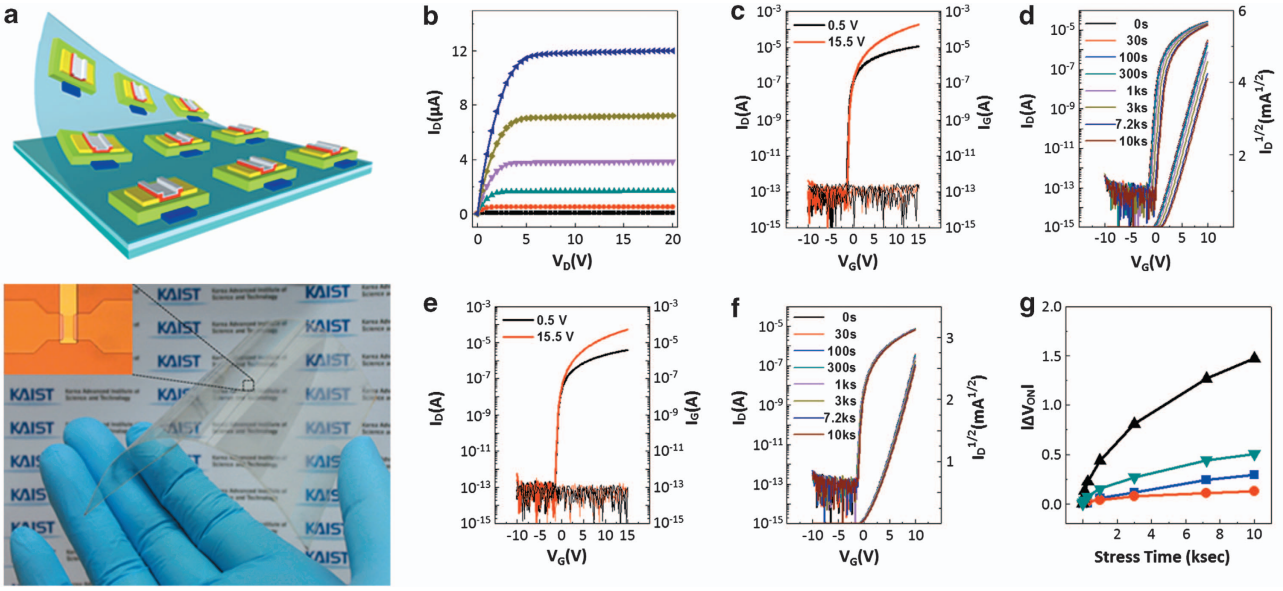

Figure 5 Transparent metal-oxide thin-film transistors (TFTs) prepared via the aqueous rate on flexible substrates. The transfer characteristics were measured with a source-drain of 15.5 and 0.5 V on flexible substrates. (**a–d)** Schematic of the device structure and optical image (**a**), output characteristics (forward and backward sweeps) (**b**), transfer characteristics (forward and backward sweeps) (**c**) and transfer characteristics with positive gate bias stress (PBS) ($V_G = 10$ V) time (**d**) of the transparent In_2O_3 TFT (annealed at 200 °C) on a flexible PEN substrate (150 nm indium tin oxide gate electrode/176 nm Al_2O_3, with 150 nm indium tin oxide source and drain electrodes, channel length, $L = 20$ μm and channel width, $W = 320$ μm). (**e**, **f**) Transfer characteristics (forward and backward sweeps) (**e**) and transfer characteristics with PBS ($V_G = 1$ V) time (**f**) of the I_7Z_3O TFT (annealed at 250 °C) on a polyimide substrate (170 nm Mo gate electrode/176 nm Al_2O_3, with 150 nm indium tin oxide source and drain electrodes, channel length, $L = 20$ μm and channel width, $W = 100$ μm). (**g**) Turn-on voltage shift (ΔV_{on}) that arises from PBS and negative gate bias stress (NBS) as a function of voltage stress time for the In_2O_3 and I_7Z_3O TFTs on plastic substrates (▲: PBS of In_2O_3 TFT, ▼:NBS of In_2O_3 TFT, ■: PBS of IZO TFT and ●: NBS of IZO TFT).

XPS analysis confirmed the compositional evolution. The resultant vacuum-post-annealed IO TFTs operated well, even under ambient annealing at 100 °C and 125 °C, with average mobilities of 0.55 and 2.42 $cm^2 V^{-1} s^{-1}$, respectively. Finally, the IO active layer was implanted onto flexible substrates. The fully transparent IO TFT on the flexible PEN substrate exhibited a mobility of 3.14 $cm^2 V^{-1} s^{-1}$ with a sub-threshold slope of 158 mV/decade and an $I_{on/off} > 10^9$. The flexible TFTs exhibited sufficient resistances to negative and positive gate bias stress, which is critical for their integrated application in devices.

CONFLICT OF INTEREST

The authors declare no conflict of interest.

ACKNOWLEDGEMENTS

This work was supported by the Materials Original Technology Program (10041222) funded by the Ministry of Knowledge Economy (MKE, Korea). This work was supported by the National Research Foundation of Korea (NRF) grant funded by the Korean government (MEST) (CAFDC- 20120000822).

Author contributions: The research was designed by YH Hwang and B-S Bae. The development of precursor solutions, the fabrication of devices and measurements were implemented by YH Hwang. The results were analyzed by YH Hwang, J-S Seo, JM Yoon, H Park and B-S Bae. The design, fabrication and measurement of transparent In_2O_3 TFT on flexible PEN substrates and IZO TFT on polyimide substrates were performed by YH Hwang, S Yang and S-H K Park. The manuscript was prepared by YH Hwang and B-S Bae. All authors examined and commented on the manuscript. The project was guided by B-S Bae.

1 Ginley, D. S., Hosono, H. & Paine, D. C. *Handbook of Transparent Conductors* 459–487 (Springer, New York, 2011).
2 Nomura, K., Ohta, H., Takagi, A., Kamiya, T., Hirano, M. & Hosono, H. Room-temperature fabrication of transparent flexible thin-film transistors using amorphous oxide semiconductors. *Nature* **432,** 488–492 (2004).
3 Kamiya, T. & Hosono, H. Material characteristics and applications of transparent amorphous oxide semiconductors. *NPG Asia Mater* **2,** 15–22 (2010).
4 Street, R. A. Thin-film transistors. *Adv. Mater.* **21,** 2007–2022 (2009).
5 Sun, Y. G. & Rogers, J. A. Inorganic semiconductors for flexible electronics. *Adv. Mater.* **19,** 1897–1916 (2007).
6 Park, S. -H. K., Hwang, C. -S., Ryu, M., Yang, S., Byun, C., Shin, J., Lee, J. -I., Lee, K., Oh, M. S. & Im, S. Transparent and photo-stable ZnO thin-film transistors to drive an active matrix organic-light-emitting-diode display panel. *Adv. Mater* **21,** 678–682 (2009).
7 Chiang, H. Q., Wager, J. F., Hoffman, R. L., Jeong, J. & Keszler, D. A. High mobility transparent thin-film transistors with amorphous zinc tin oxide channel layer. *Appl. Phys. Lett.* **86,** 013503 (2005).
8 Mitzi, D. B. *Solution Processing of Inorganic Materials* 1–32 (Wiley, New Jersey, 2009).
9 Arias, A. C., MacKenzie, J. D., McCulloch, I., Rivnay, J. & Salleo, A. Materials and applications for large area electronics: solution-based approaches. *Chem. Rev.* **110,** 3–24 (2010).
10 Lee, D. H., Chang, Y. J., Herman, G. S. & Chang, C. H. A general route to printable high-mobility transparent amorphous oxide semiconductors. *Adv. Mater.* **19,** 843–847 (2007).
11 Adamopoulos, G., Bashir, A., Thomas, S., Gillin, W. P., Georgakopoulos, S., Shkunov, M., Baklar, M. A., Stingelin, N., Maher, R. C., Cohen, L. F., Bradley, D. D. C. & Anthopoulos, T. D. Spray-deposited Li-doped ZnO transistors with electron mobility exceeding 50 cm^2/Vs. *Adv. Mater.* **22,** 4764–4769 (2010).
12 Choi, C. G., Seo, S. -J. & Bae, B. -S. Solution-processed indium-zinc oxide transparent thin-film transistors. *Electrochem. Solid-State Lett.* **11,** H7–H9 (2008).
13 Meyers, S. T., Anderson, J. T., Hung, C. M., Thompson, J., Wager, J. F. & Keszler, D. A. Aqueous inorganic inks for low-temperature fabrication of ZnO TFTs. *J. Am. Chem. Soc.* **130,** 17603–17609 (2008).
14 Banger, K. K., Yamashita, Y., Mori, K., Peterson, R. L., Leedham, T., Rickard, J. & Sirringhaus, H. Low-temperature, high-performance solution-processed metal oxide thin-film transistors formed by a 'sol-gel on chip' process. *Nat. Mater* **10,** 45–50 (2011).
15 Kim, M. G., Kanatzidis, M. G., Facchetti, A. & Marks, T. J. Low-temperature fabrication of high-performance metal oxide thin-film electronics via combustion processing. *Nat. Mater.* **10,** 382–388 (2011).

16 Hwang, Y. H., Jeon, J. H. & Bae, B. -S. Post-humid annealing of low-temperature solution-processed indium based metal oxide thin-film transistors. *Electrochem. Solid-State Lett.* **14,** H303–H305 (2011).
17 Sun, B. & Sirringhaus, H. Solution-processed zinc oxide field-effect transistors based on self-assembly of colloidal nanorods. *Nano Lett* **5,** 2408–2413 (2005).
18 Eda, G., Fanchini, G. & Chhowalla, M. Large-area ultrathin films of reduced graphene oxide as a transparent and flexible electronic material. *Nat. Nanotech* **3,** 270–274 (2008).
19 Livage, J., Henry, M. & Sanchez, C. Sol-gel chemistry of transition metal oxide. *Prog. Solid St. Chem.* **18,** 259–341 (1988).
20 Brinker, C. J. & Scherer, G. W. *Sol-Gel Science: The Physics and Chemistry of Sol-Gel Processing* 21–78 (Academic Press, London, 1990).
21 Kozhevnikova, G. V. & Keresztury, G. The state of indium ions in nitrate solutions: a Raman spectroscopic study. *Inorganica Chim. Acta.* **98,** 59–65 (1985).
22 Samsonenko, D. G., Sokolov, M. N., Virovets, A. V., Pervukhina, N. V. & Fedin, V. P.Isolation and structural characterization of new indium aqua complexes: trans-$[InCl_2(H_2O)_4]^+$ and trans-$[InCl_4(H_2O)_2]^-$ as supramolecular adducts with cucurbituril and related studies. *Eur. J. Inorg. Chem.* **2001,** 167–172 (2001).
23 Scherer, G. W. Sintering of sol-gel films. *J. Sol-Gel Sci. Tech* **8,** 353–363 (1997).
24 Jeong, S., Ha, Y. G., Moon, J., Facchetti, A. & Marks, T. J. Role of gallium doping in dramatically lowering amorphous-oxide processing temperatures for solution-derived indium zinc oxide thin-film transistors. *Adv. Mater.* **22,** 1346–1350 (2010).
25 Fan, J. C. C. & Goodenough, J. B. X-ray photoemission spectroscopy studies of Sn-doped indium-oxide films. *J. Appl. Phys.* **48,** 3524–3531 (1977).
26 Moulder, J. F., Stickle, W. F., Sobol, P. E. & Bomben, K. D. *Handbook of X-ray Photoelectron Spectroscopy* 1–261 (Physical Electronics, Minnesota, 1992).
27 Kim, H. S., Kim, M. -G., Ha, Y. -G., Kanatzidis, M. G., Marks, T. J. & Facchetti, A. Low-temperature solution-processed amorphous indium tin oxide field-effect transistors. *J. Am. Chem. Soc.* **131,** 10826–10827 (2009).
28 Hwang, Y. H., Jeon, J. H., Seo, S. -J. & Bae, B. -S. Solution-processed, high-performance aluminum indium oxide thin-film transistors fabricated at low temperature. *Electrochem. Solid-State Lett.* **12,** H336–H339 (2009).
29 Seo, S. -J., Hwang, Y. H. & Bae, B. -S. Post-annealing process for low temperature processed sol-gel zinc tin oxide thin film transistors. *Electrochem. Solid-State Lett* **13,** H357–H359 (2010).
30 Zhu, M., Huang, H., Gong, J., Sun, C. & Jiang, X. Role of oxygen desorption during vacuum annealing in the improvement of electrical properties of aluminum doped zinc oxide films synthesized by sol gel method. *J. Appl. Phys.* **102,** 043106 (2007).
31 Jeong, J. K., Jeong, J. H., Yang, H. W., Park, J. -S., Mo, Y. -G. & Kim, H. D. High performance thin film transistors with cosputtered amorphous indium gallium zinc oxide channel. *Appl. Phys. Lett.* **91,** 113505 (2007).

Supplementary Information accompanies the paper on the NPG Asia Materials website (http://www.nature.com/am)